ARTICLE

Population pharmacokinetic and pharmacodynamic analysis of rivaroxaban in Chinese patients with non-valvular atrial fibrillation

Xiao-qin Liu[1], Yu-fei Zhang[1], Hong-yan Ding[2], Ming-ming Yan[1], Zheng Jiao[1,3], Ming-kang Zhong[1] and Chun-lai Ma[1]

Rivaroxaban, a direct factor Xa inhibitor, is widely used for stroke prevention in patients with non-valvular atrial fibrillation (NVAF). The aim of this study was to conduct a population pharmacokinetic-pharmacodynamic (PK-PD) analysis of rivaroxaban in Chinese patients with NVAF to assess ethnic differences and provide model-based precision dosing. A total of 256 rivaroxaban plasma concentrations and 244 prothrombin time (PT) measurements were obtained from 195 Chinese NVAF patients from a prospective clinical trial. The population PK-PD model was developed using nonlinear mixed effects modeling (NONMEM) software. The PK of rivaroxaban was adequately described using a one-compartment model with first-order adsorption and elimination. Estimated glomerular filtration rate (eGFR) was identified as a major covariate for apparent clearance. No single nucleotide polymorphism was identified as a significant covariate. PT exhibited a linear relationship with rivaroxaban concentration. Total bilirubin (TBIL) and eGFR were identified as significant covariates for baseline PT. According to the Monte Carlo simulation, 15 mg for Chinese patients with eGFR ≥50 mL/min and normal liver function yielded an exposure comparable to 20 mg for Caucasian patients. Patients with moderately impaired renal function may require a lower dose of rivaroxaban to avoid overexposure. Moreover, there was an approximate 26% increase in PT levels in patients with TBIL of 34 μmol/L and eGFR of 30 mL/min, which could increase the risk of major bleeding. The established population PK-PD model could inform individualized dosing for Chinese NVAF patients who are administered rivaroxaban.

Keywords: rivaroxaban; atrial fibrillation; population pharmacokinetics-pharmacodynamics; model-informed precision dosing; Chinese

INTRODUCTION

Atrial fibrillation (AF) is one of the most common cardiovascular diseases and has caused considerable economic burden worldwide [1, 2]. Rivaroxaban is an available non-vitamin K antagonist oral anticoagulant (NOAC), which directly inhibits the activity of factor Xa [3]. It has been widely used to prevent stroke in patients with non-valvular atrial fibrillation (NVAF) [4, 5].

Following oral administration, rivaroxaban is rapidly absorbed and reaches the maximum plasma concentration after 2–4 h [6, 7]. For doses greater than 10 mg, taking rivaroxaban with food is necessary to increase bioavailability [8]. Rivaroxaban has a high plasma protein binding (92%–95%) and a mean volume of distribution of 0.62 L/kg [3]. Approximately two-thirds of rivaroxaban is metabolized by the liver, and hepatic cytochrome P450 enzymes (CYP) 3A4/5 account for ~18% of rivaroxaban metabolism [3, 9]. Another one-third of rivaroxaban is eliminated unchanged in the urine, primarily via active renal secretion [3, 9]. P-glycoprotein and breast cancer resistance protein (BCRP), encoded respectively by the ATP-binding cassette sub-family B member (*ABCB1*) gene and ATP-binding cassette sub-family G member (*ABCG2*), are the main transporters involved in the process of active renal secretion [9, 10].

Twenty milligrams every 24 h (q24h) as a standard dose for NVAF patients with creatinine clearance (CrCl) ≥50 mL/min and 15 mg q24h for patients with CrCl 30–49 mL/min were recommended by the Food and Drug Administration (FDA) of the United States [9], the National Medical Products Administration (NMPA) of China, as well as "guideline of stroke prevention in Chinese patients with AF" [11]. However, a lower rivaroxaban dose (15 mg for CrCl ≥50 mL/min or 10 mg for CrCl 30–49 mL/min) was approved for Japanese patients by the Pharmaceuticals and Medical Devices Agency of Japan. On the one hand, a higher exposure in Japanese patients was observed compared to Caucasian patients at the same dose [12–15]. On the other hand, the efficacy and safety of the lower dose for Japanese patients was demonstrated in a phase III clinical trial of J-ROCKET AF compared with the non-Japanese trial of ROCKET AF [12, 16].

Recent studies conducted in Korea and China Taiwan, China demonstrated that a lower rivaroxaban dose was associated with a lower risk of thromboembolic events, intracranial hemorrhage, and all-cause mortality in contrast to those administered warfarin

---

[1]Department of Pharmacy, Huashan Hospital, Fudan University, Shanghai 200040, China; [2]Department of Neurology, Huashan Hospital, Fudan University, Shanghai 200040, China and [3]Department of Pharmacy, Shanghai Chest Hospital, Shanghai Jiao Tong University, Shanghai 200030, China
Correspondence: Ming-kang Zhong (mkzhong_hs@126.com) or Chun-lai Ma (chunlaima@126.com)

SPRINGER NATURE

[17–19]. Moreover, compared to the standard 15 mg dose, a lower dose of 10 mg was associated with a lower risk of major bleeding in patients with impaired renal function [20, 21]. However, thus far, little is known about the pharmacokinetic-pharmacodynamic (PK-PD) characteristics regarding the optimal dosage of rivaroxaban in Chinese NVAF patients in a real clinical setting.

Therefore, a prospective clinical study was conducted to develop a population PK-PD model of rivaroxaban in Chinese patients with NVAF to (i) evaluate the ethnic differences in PK among Chinese, Caucasian, and Japanese populations; (ii) assess the effect of renal function and other potential variables on the PK and PD of rivaroxaban; and (ii) provide individualized dosing strategies for Chinese patients using the established model.

MATERIALS AND METHODS

Study design
A prospective, single-center clinical study was conducted at Huashan Hospital, Fudan University, China (https://www.chictr.org.cn/index.aspx, ChiCTR2100046685). Patients diagnosed with NVAF using an electrocardiogram according to the 2016 European Heart Rhythm Association Guidelines [22] and receiving rivaroxaban for at least 3 continuous doses were recruited in this study from September 1, 2020, to June 30, 2021. Patients were excluded if they exhibited at least one of the following: (1) moderate or severe liver dysfunction (Child–Pugh classification B or C [23]); (2) severe renal dysfunction (CrCl calculated using the Cockcroft-Gault formula [24] <15 mL/min); (3) pregnancy; (4) history of malignant tumor; or (5) spontaneous bleeding tendency, such as coagulation disorder or thrombocytopenia (blood platelet count $<20 \times 10^9$/L).

Patient demographics and laboratory test results were collected. Other data collected included the dosing histories of concomitant drugs that inhibit or induce CYP450 3A enzymes and drug transport systems and may change the exposure of rivaroxaban as listed in the FDA label. These drugs included ketoconazole, ritonavir, clarithromycin, erythromycin, carbamazepine, rifampin, St. John's wort, enoxaparin, warfarin, aspirin, clopidogrel, other platelet aggregation inhibitors, or non-steroidal anti-inflammatory drugs. The rivaroxaban dose amount and dosing time were also recorded for each participant. CHA2DS2-VASc (congestive heart failure, hypertension, age, diabetes, previous stroke/transient ischemic attack, vascular disease, sex category) scores [25] and HAS-BLED (hypertension, abnormal liver/renal function, stroke history, bleeding history or predisposition, labile INR, elderly, drug/alcohol usage) scores [26] were calculated to assess the risk of thromboembolism and bleeding.

Blood samples from inpatients were collected before (defined as trough samples), 3 ± 0.5 h (defined as peak samples) and 7 ± 0.5 h after at least three continuous doses, according to the design of previous studies [14, 27]. Blood samples from outpatients were collected opportunistically. The timing of dosing and sampling was recorded for each patient.

At each sampling, 2.7 mL blood samples were collected into trisodium citrate-containing tubes for measurement of prothrombin time (PT). Another 2 mL of blood was collected into ethylenediaminetetraacetic acid-containing tubes for measurement of rivaroxaban plasma concentration and extraction of genomic DNA. Samples were centrifuged at $3000 \times g$ for 10 min at 20 °C within 4 h of sample collection. All samples were stored at −80 °C and analyzed within 3 months.

This study followed the principles of the Declaration of Helsinki (2013) and was approved by the Ethics Committee of Huashan Hospital (KY2020-016). Informed consent was obtained from all the participants prior to enrollment.

Bioassay
A sensitive ultra-performance liquid chromatography with tandem mass spectrometry method was used to measure the rivaroxaban plasma concentration [28]. The lower limit of quantitation was 1 µg/L, and the calibration range of this assay was 1–1000 µg/L. The inter- and intra-accuracies were 85.9%–114%, and intra- and inter-day precision was less than 10%.

PT was measured with Thromborel® S (Siemens, Marburg, Germany) using a CN6000 coagulation analyzer (Sysmex, Kobe, Japan). The reported range was 0–170 s. The within-run and inter-run precision was <3% [29].

Genotyping
Single nucleotide polymorphisms (SNPs) for four genes involved in the PK of rivaroxaban—*ABCB1*, *ABCG2*, *CYP3A4*, and *CYP3A5*—were collected from the 1000 Genome Project (https://www.ncbi.nlm.nih.gov/variation/tools/1000genomes/) and the dbSNP database of the National Center for Biotechnology Information (NCBI) (https://www.ncbi.nlm.nih.gov/snp/) and analyzed using Haploview software (version 4.20, https://www.broadinstitute.org/haploview/haploview). Candidate SNPs were included in the analysis according to the following criteria: (i) the minor allele frequency was >20% and (ii) alleles identified by the tests had an r^2 threshold of 0.8, as the default in the Haploview software, and have also been commonly used in previous studies [30, 31].

Genomic DNA was extracted using a TIANGEN DNA Kit (DP348, TIANGEN Biotech, Beijing, China) according to the manufacturer's protocol. Genotypes were analyzed using the MALDI-TOF MassArray assay by Shanghai Benegene Biotechnology Co., Ltd. (Shanghai, China). The exact test for Hardy-Weinberg equilibrium was performed using the *HardyWeinberg* package (version 1.7.2) in R software (version 4.1.1, R Foundation for Statistical Computing, Vienna, Austria).

Population pharmacokinetic-pharmacodynamic modeling
Population PK-PD analysis was performed using non-linear mixed-effects modeling (NONMEM®, version 7.4.2; ICON Development Solutions, Ellicott City, MD, USA) with first-order conditional estimation with interaction method. The evaluation of the NONMEM output, statistical analysis, and diagnostic plots was performed using R software and Pirana software (version 2.9.7, Certara, Inc., NJ, USA).

Compared to the "gold standard" simultaneous modeling method, a sequential modeling strategy is more time-saving, and estimates are also more likely to be obtained [32, 33]. Therefore, the sequential modeling strategy was first applied to the development of the population PK model, and then individual empirical Bayesian estimates of PK parameters were used as input for the second stage of sequential PD modeling. Finally, a linked population PK-PD model was applied to estimate all PK-PD parameters simultaneously and to compare the parameter estimates via a sequential modeling strategy.

Population pharmacokinetic modeling
Base model: One-compartment and two-compartment models were tested as candidate structural models. The base model including bodyweight with allometric scaling was also tested, according to a previous pooled population PK studies based on 4918 patients [34], as well as classical allometric scaling (0.75 for apparent clearance (CL/F), and 1 for apparent volume of distribution (V/F)) [35], which considered bodyweight as a significant covariate for both CL/F and V/F. The selection of the structural model was based on the Akaike information criterion, Bayesian information criterion, condition number, and precision of estimates. An exponential model for between-subject variability (BSV) was applied to the PK parameters in below equation:

$$P_i = P_{pop} \cdot e^{\eta_i} \tag{1}$$

where and P_i represents the individual parameter estimate of the ith patient, P_{pop} represents the typical population parameter

Population PK-PD of rivaroxaban in NVAF patients
XQ Liu et al.

2725

estimate, η_i is normally distributed with a mean of zero and variance of ω^2.

Residual unexplained variability (RUV) was tested using an additive (Eq. (2)), proportional (Eq. (3)) or combined models (Eq. (4)):

$$Y = IPRED + \varepsilon_1 \tag{2}$$

$$Y = IPRED \cdot (1 + \varepsilon_2) \tag{3}$$

$$Y = IPRED \cdot (1 + \varepsilon_2) + \varepsilon_1 \tag{4}$$

where Y represents the observation, $IPRED$ represents the individual predicted concentration, and ε_1 and ε_2 represent the additive and proportional error components, respectively, which are assumed to be normally distributed with a mean of zero and variance of σ^2.

Covariate model: Potential covariates were tested, including age, sex, body weight, body surface area, lean body mass, white blood cell count, red blood cell count, hemoglobin (HGB), hematocrit, platelet count, aspartate aminotransferase, alanine aminotransferase, total bilirubin (TBIL), direct bilirubin, alkaline phosphatase, albumin, gamma-glutamyl transpeptidase, urea nitrogen, urea acid, serum creatinine, CrCl, and eGFR (calculated using the Chronic Kidney Disease Epidemiology Collaboration formula [36]). For concomitant drugs, only those with a comedication rate >15% were tested. Continuous covariates were tested using a proportional (Eq. (5)), exponent (Eq. (6)), or power (Eq. (7)) model.

$$P_i = P_{pop} \cdot \left(1 + \theta \cdot \frac{COV}{COV_{median}} \right) \tag{5}$$

$$P_i = P_{pop} \cdot \left(\frac{COV}{COV_{median}} \right)^{\theta} \tag{6}$$

$$P_i = P_{pop} \cdot e^{\theta \cdot (COV - COV_{median})} \tag{7}$$

where COV and COV_{median} represent the individual and median values of a covariate, respectively, θ represents the estimated value of the covariate effect.

Categorical covariates, such as SNPs, were tested using a scale model (Eq. (8)).

$$P_i = \begin{cases} P_{pop} \, (if \ homozygous \ wild \ type \ carriers) \\ P_{pop} \cdot \theta_1 \, (if \ heterozygous \ mutation \ carriers) \\ P_{pop} \cdot \theta_2 \, (if \ homozygous \ mutation \ carriers) \end{cases} \tag{8}$$

where θ_1 and θ_2 represent the change of typical values with heterozygous mutation carriers and homozygous mutation carriers compared to homozygous wild-type carriers, respectively. Each SNP was tested individually. Besides, dominant model and recessive model were also tested.

The covariate model was built using a stepwise forward inclusion and backward elimination process. The criteria for covariate selection included a decrease in objective function value (OFV) > 3.84 ($df = 1$, $P < 0.05$) in the forward selection step and an increase in OFV > 6.63 ($df = 1$, $P < 0.01$) in the backward elimination step. For continuous variables, if PK parameter estimates calculated with the maximum or minimum of the covariate changed less than 20% relative to the population PK estimate, the effect of covariates was not considered clinically relevant. Similarly, if PK parameter estimates in the presence of the categorical variable changed less than 20% relative to the population PK estimate, it was also not clinically relevant. The selection of covariate model also considered the physiological plausibility and goodness-of-fit (GOF) plots.

Population pharmacodynamic modeling. Individual PK parameters were estimated using the POSTHOC method with the established population PK model to develop the population PD model. Structural models were assessed using a linear (Eq. (9)) or near-linear (Eqs. (10, 11)) model, according to previous studies [14, 27, 37].

$$PT = PT_{base} + slope \times C_p \tag{9}$$

$$PT = PT_{base} + slope \times C_p^{hill} \tag{10}$$

$$PT = PT_{base} + slope \times C_p^{1 - hill \times C_p} \tag{11}$$

where PT_{base} represents the baseline of PT, C_p represents the rivaroxaban plasma concentration, *slope* represents the change in PT resulting from the change per unit concentration, and *hill* represents the exponent of C_p.

BSV was tested using an exponential (Eq. (1)) or additive (Eq. (12)) model.

$$P_i = P_{pop} + \eta_i \tag{12}$$

The RUV was tested using an additive (Eq. (2)), proportional (Eq. (3)) or combined model (Eq. (4)). The method for selection of the structural model, covariate screening, and selection criteria of covariates were the same as those in the development of the population PK model. The effect of SNPs was not tested in the PD model, because they all referred to transporters or drug-metabolizing enzymes in the PK process and had no direct effect on PD.

Model evaluation. The performance of the final model was evaluated using diagnostic GOF plots, including observed values (DV) *versus* population predicted values (PRED), DV *versus* individual predicted values (IPRED), conditional weighted residuals (CWRES) versus PRED, and CWRES *versus* time after last dose.

The robustness of the final model was evaluated using nonparametric bootstrap resampling ($n = 2000$). The median and 2.5th–97.5th percentiles of parameter estimates from the resampled datasets were calculated and compared with the final parameter estimates.

The visual predictive check (VPC) approach was used to evaluate the predictive performance of the model based on simulations ($n = 1000$). The median and 5th–95th percentiles of the observed data with the corresponding simulated data were compared. The consistency of variability and the central tendency between the observed and simulated data were visually assessed.

Bootstrap and VPC analyses were performed using Perl-speaks-NONMEM software (PsN, version 4.6.0, Department of Pharmaceutical Biosciences, Uppsala University, Sweden, https://uupharmacometrics.github.io/PsN/index.html).

Model-informed precision dosing
Monte Carlo simulations were employed to compare PK exposure by ethnic groups based on the established population PK model, as well as the reports from a Caucasian NVAF population [27] and Japanese NVAF population [15]. The area under the concentration-time curve over 24 h at steady state ($AUC_{24,ss}$) was estimated for Caucasian, Japanese and Chinese patients taking 10, 15 or 20 mg q24h, as shown in below equation.

$$AUC_{24,ss} = \frac{DOSE(mg)}{CL/F(L/h)} \tag{13}$$

In each model, 1000 simulations were performed based on three typical patients, who had normal, mildly impaired, and moderately impaired renal function, respectively.

Furthermore, simulations were employed based on the final population PK-PD model to evaluate the effect of covariates on the PK and PD of rivaroxaban at various dosing levels. Rivaroxaban

Population PK-PD of rivaroxaban in NVAF patients
XQ Liu et al.

2726

Table 1. Baseline patient characteristics.

Variables	Median (range)/count	Mean ± SD
Number of patients (male/female)	195 (111/84)	
Number of rivaroxaban concentration samples	256	
Number of prothrombin time samples	244	
Age (year)	68 (28–96)	66.7 ± 11.7
Body weight (kg)	68 (36.5–119)	68.9 ± 12.9
Body surface area[a] (m^2)	1.78 (1.19–2.42)	1.78 ± 0.20
Lean body weight[b] (kg)	51.81 (29–73.29)	51.45 ± 8.90
Daily dose (mg)	15 (5–20)	15.7 ± 3.9
CHAS2DS2-VASc score[c]	3 (0–7)	2.72 ± 1.70
HAS-BLED score[d]	2 (0–7)	2.37 ± 1.21
White blood cells count (10^9/L)	6.05 (2.71–14.21)	6.39 ± 2.09
Red blood cells count (10^9/L)	4.35 (1.38–6.19)	4.33 ± 0.67
Hemoglobin (g/L)	133 (62–198)	134.14 ± 21.08
Hematocrit (%)	39.8 (20.3–53.4)	39.58 ± 5.34
Platelet count (10^9/L)	193 (74–385)	194.55 ± 58.41
Alanine aminotransferase (U/L)	21 (3–204)	27.01 ± 21.96
Aspartate aminotransferase (U/L)	21 (8–75)	23.68 ± 11.16
Total bilirubin (μmol/L)	11.6 (3.3–63.3)	14.41 ± 9.19
Direct bilirubin (μmol/L)	3.6 (0.2–31.6)	5.01 ± 4.39
Alkaline phosphatase (U/L)	71 (12–387)	75.96 ± 35.45
Gamma-glutamyl transpeptidase (U/L)	32 (10–338)	50.15 ± 52.31
Total protein (g/L)	65 (49–88)	65.58 ± 6.43
Albumin (g/L)	40 (30–50)	39.92 ± 4.08
Urea (mmol/L)	6 (2.4–23.2)	6.42 ± 2.45
Uric acid (mmol/L)	0.366 (0.104–0.91)	0.38 ± 0.13
Serum creatinine (mg/dL)	0.92 (0.25–2.85)	0.95 ± 0.32
Estimated glomerular filtration rate (mL/min)[e]	79.7 (21.85–127.73)	77.82 ± 21.18

[a] body surface area$(m^2) = \sqrt{height \times weight/3600}$;.
[b]Lean body mass (kg) = 1.1 × weight-128 × weight^2/height^2 (male); lean body mass (kg) = 1.07 × weight-148 × weight^2/height^2 (female);
[c]CHA2DS2-VASc score: congestive heart failure or left ventricular systolic dysfunction (1 point); hypertension (1 point); age 65–74 years (1 point) or ≥75 years (2 points); diabetes mellitus (1 point); prior stroke or TIA thromboembolism (2 points); vascular disease (1 point); female (1 point).
[d]HAS-BLED score: hypertension (1 point); liver disease (1 point); renal disease (1 point); stroke history (1 point); prior major bleeding or predisposition to bleeding (1 point); labile INR (1 point); age >65 years (1 point); medication usage predisposing to bleeding (1 point); alcohol use (1 point).
[e]Estimated glomerular filtration rate (eGFR, mL/min) was calculated by the Chronic Kidney Disease Epidemiology Collaboration equation: for male with SCr (serum creatinine) ≤ 0.9 mg/dL: eGFR = 141 × (SCr/0.9)$^{-0.411}$ × 0.933^{age}; for male with SCr > 0.9 mg/dL: eGFR = 141 × (SCr/0.9)$^{-1.209}$ × 0.933^{age}; for female with SCr ≤ 0.7 mg/dL: eGFR = 144 × (SCr/0.7)$^{-0.329}$ × 0.933^{age}; for female with SCr > 0.7 mg/dL: eGFR = 144 × (SCr/0.7)$^{-1.209}$ × 0.933^{age}.

Table 2. Frequency of distribution of genetic polymorphisms.

Gene	SNP	Variants	Count	Percentage (%)	P value
ABCB1					
	rs1045642	AA/AG/GG	19/102/74	9.7/52.3/37.9	0.064
	rs1128503	AA/AG/GG	83/97/15	42.6/49.7/7.7	0.074
	rs4148738	CC/CT/TT	27/102/66	13.8/52.3/33.8	0.236
	rs868755	GG/GT/TT	60/106/29	30.8/54.4/14.9	0.141
	rs2235035	AA/GA/GG	12/91/92	6.2/46.7/47.2	0.120
ABCG2					
	rs1448784	AA/AG/GG	96/81/18	49.2/41.5/9.2	0.865
	rs2231137	CC/TC/TT	81/87/27	41.5/44.6/13.8	0.643
	rs2231142	GG/GT/TT	86/87/22	44.1/44.6/11.3	1.000
	rs3114018	AA/CA/CC	30/90/75	15.4/46.2/38.5	0.762
CYP3A4					
	rs2246709	AA/GA/GG	74/84/37	37.9/43.1/19	0.139
	rs2242480	CC/CT/TT	108/77/10	55.4/39.5/5.1	0.565
	rs3735451	CC/CT/TT	15/75/105	7.7/38.5/53.8	0.719
	rs4646440	AA/GA/GG	10/68/117	5.1/34.9/60	1.000
CYP3A5					
	rs776746	CC/TC/TT	111/67/17	56.9/34.4/8.7	0.139

SNP single nucleotide polymorphism.

The range of the 5th–95th percentiles of AUC$_{24,ss}$ and PT$_{ave,ss}$ for a typical patient was set as the reference range. The optimal dose for patients with different levels of covariates was defined as the dose at which PT$_{ave,ss}$ and AUC$_{24,ss}$ falls within the reference range in maximum proportion as estimated from the established PK-PD model.

RESULTS

Study population

Data from 195 patients were collected in this study, with 256 concentration measurements and 244 PT measurements available for PK-PD modeling. Approximately 70% and 17% of the samples were collected before and 3 ± 0.5 h after administration, respectively. Patient demographics are shown in Table 1. The prescribed daily dose ranged from 5 to 20 mg. The eGFR ranged from 22 to 128 mL/min, and 24.6% of the patients had an eGFR of 15–50 mL/min. Median CHA2DS2-VASc score and HAS-BLED score were 2.7 and 2.4, respectively. All participants were administered rivaroxaban with food. None of the investigated medications accounted for >15% of the patients.

By screening 1000 Genome Project and the dbSNP database of NBCI, identified SNPs included *ABCB1* 3435 C>T (rs1045642), 1236 C>T (rs1128503), 2677 G>T/A (rs2032582), rs2235035, rs4148738, and rs868755; *ABCG2* rs1448784, rs2231137, rs2231142, and rs3114018; *CYP3A4* rs2242480, rs2246709, rs3735451, and rs4646440; and *CYP3A5**3 (rs776746). Primer sequences for SNPs were shown in Supplementary Table S1. *ABCB1* rs2032582 failed the Hardy-Weinberg equilibrium test (*P* < 0.05); thus, it was excluded from further analysis. Genotype distribution and allele frequencies of the included SNPs are shown in Table 2. The minor allele frequencies of other SNPs were consistent with those reported in the dbSNP database of NCBI.

Population pharmacokinetic-pharmacodynamic model

Population pharmacokinetic model. The PK of rivaroxaban was described by a one-compartment model with first-order absorption and elimination. Allometric scaling factors were not included in the model because they could not be precisely estimated

concentration-time and PT-time distribution under different dosing strategies to match the exposure of patients at different levels of covariates were simulated to estimate AUC$_{24,ss}$ and average PT at steady state (PT$_{ave,ss}$) for each group (n = 1000). AUC$_{24,ss}$ was calculated using Eq. (13), and PT$_{ave,ss}$ was calculated according to its relationship with the average concentration at steady state (C$_{ave,ss}$), as shown in Eq. (14), where C$_{ave,ss}$ is calculated using Eq. (15).

$$PT_{ave,ss} = f(C_{ave,ss}) \tag{14}$$

$$C_{ave,ss} = AUC_{24,ss}/24 \tag{15}$$

Population PK-PD of rivaroxaban in NVAF patients
XQ Liu et al.

2727

Table 3. Population parameter estimates for the pharmacokinetic-pharmacodynamic model.

Parameters	Sequential modeling		Simultaneous modeling		Bootstrap [a]	
	Estimates (%RSE)	Shrinkage (%)	Estimates (%RSE)	Shrinkage (%)	Median	2.5%–97.5% CI
PK						
k_a (h^{-1})	0.617 (fixed)	/	0.617 (fixed)	/	/	/
CL/F (L/h)	5.04 (5)	/	5.03 (5)	/	5.04	4.56–5.57
eGFR on CL/F	0.54 (16)	/	0.53 (17)	/	0.53	0.35–0.72
V/F (L)	40.4 (6)	/	40.3 (7)	/	40.3	35.5–46.6
Between-subject variability (%CV)						
ω_{CL}	35.4 (6)	8	35.4 (6)	8	35.1	30.5–39.5
Residual unexplained variability (%CV)						
Proportional error	33.6 (13)	29	33.6 (13)	29	33.4	28.9–37.4
PT						
PT_{base} (s)	13.9 (4)	/	13.9 (4)	/	13.9	12.8–15.0
TBIL on PT_{base}	0.00581 (16)	/	0.00574 (16)	/	0.00569	0.00359–0.00742
eGFR on PT_{base}	−0.0868 (39)	/	−0.0872 (39)	/	−0.0877	(−0.1532)–(−0.0132)
slope (s·L·µg^{-1})	0.0132 (10)	/	0.0133 (10)	/	0.0133	0.0105–0.0159
Between-subject variability (%CV)						
$\omega_{PT_{base}}$	6.1 (30)	51	5.6 (38)	55	5.7	1.6–8.3
ω_{slope}	62.4 (16)	49	61.8 (16)	50	60.6	35.5–83.3
Residual unexplained variability (%CV)						
Proportional error	9.4 (19)	21	9.4 (18)	21	9.2	7.4–10.7

CL/F the apparent clearance, *eGFR* estimated glomerular filtration rate, *k_a* the absorption rate, *PT* prothrombin time, *PT_{base}* baseline of PT, *TBIL* total bilirubin, *V/F* the apparent volume of distribution.
Notes: a. bootstrap was based on the final model by simultaneous modeling.
$CL/F = 5.03 \times (eGFR/80)^{0.53}$.
$PT = 13.9 \times e^{0.00574 \times (TBIL-12)} \times [1 - 0.0872 \times (eGFR/80)] + 0.0133 \times C_p$ (C_p represents rivaroxaban plasma concentration).

(relative standard error (%RSE) > 130%). Because of the limited samples in the absorption phase, a previously reported k_a of 0.617 h^{-1} was applied in this study [15]. In addition, because the majority of the samples were collected before dosing, the BSV of V/F could not be estimated precisely and thus was removed. Of the tested RUV models, an additive RUV model had the highest OFV; a combined RUV model had a similarly lower OFV with a proportional model, and the additive error of the combined RUV could not be estimated precisely (%RSE=187%). Therefore, a proportional RUV model was adopted for the rivaroxaban concentration.

In the forward inclusion step, eGFR, *ABCB1* rs4148738, and *CYP3A4* rs2246709 were shown to significantly affect CL/F. In the backward elimination step, the effect of *CYP3A4* rs2246709 was removed because of an increase in OFV < 6.63 (Supplementary Table S2). Moreover, the effect of *ABCB1* rs4148738 on CL/F was only 19% on CL/F, which was not considered clinically relevant. Therefore, only the effect of the eGFR was retained. The BSV of V/F was not estimated, and no covariates were screened based on V/F. The estimates of the established population PK model parameters are presented in Table 3. The OFV of the final population PK model was 2211.533, with a decrease of 35.058 compared with the base model.

Population pharmacodynamic model. A linear model (Eq. (9)) described the relationship between rivaroxaban PK and PT, whereas near-linear models as Eqs. (10) and (11) failed to fit the data because of the %RSE of *slope* or *hill* > 100%. An exponential BSV model and proportional RUV model were applied to the PT model. In the forward inclusion step, the model with TBIL, eGFR, and HGB was successively detected as having significant covariates for PT_{base}. In the backward elimination step, HGB was

removed by an increase in OFV < 6.63 (P < 0.01) (Supplementary Table S3). The OFV dropped from 582.25 in the base model to 534.86 in the final model. The estimates of the PD model parameters are presented in Table 3.

Population pharmacokinetic-pharmacodynamic model. A simultaneous modeling strategy was successfully applied to fit all the PK and PD data. The estimates of the linked population PK-PD model parameters are listed in Table 3. The difference in parameter estimates between the two modeling strategies was less than 9%. There was a drop in OFV of 85.72 in the final population PK-PD model compared to that in the base model.

The equations for CL/F and PT are as shown in below equations.

$$CL/F(L/h) = 5.03 \times \left(\frac{eGFR}{80}\right)^{0.53} \tag{16}$$

$$PT = 13.9 \times e^{0.00574 \times (TBIL-12)} \times \left[1 - 0.0872 \times \left(\frac{eGFR}{80}\right)\right] + 0.0133 \times C_p \tag{17}$$

where C_p represents rivaroxaban plasma concentration.

Model evaluation. Diagnostic GOF plots for population PK and PD models are shown in Figs. 1 and 2, respectively. The predicted and observed rivaroxaban plasma concentrations and PT levels showed adequate agreement over the whole range. No obvious bias or trends are shown in scatterplots of CWRES *versus* time after last dose and CWRES *versus* PRED.

The robustness of the linked population PK-PD model was evaluated using a nonparametric bootstrap method. The median
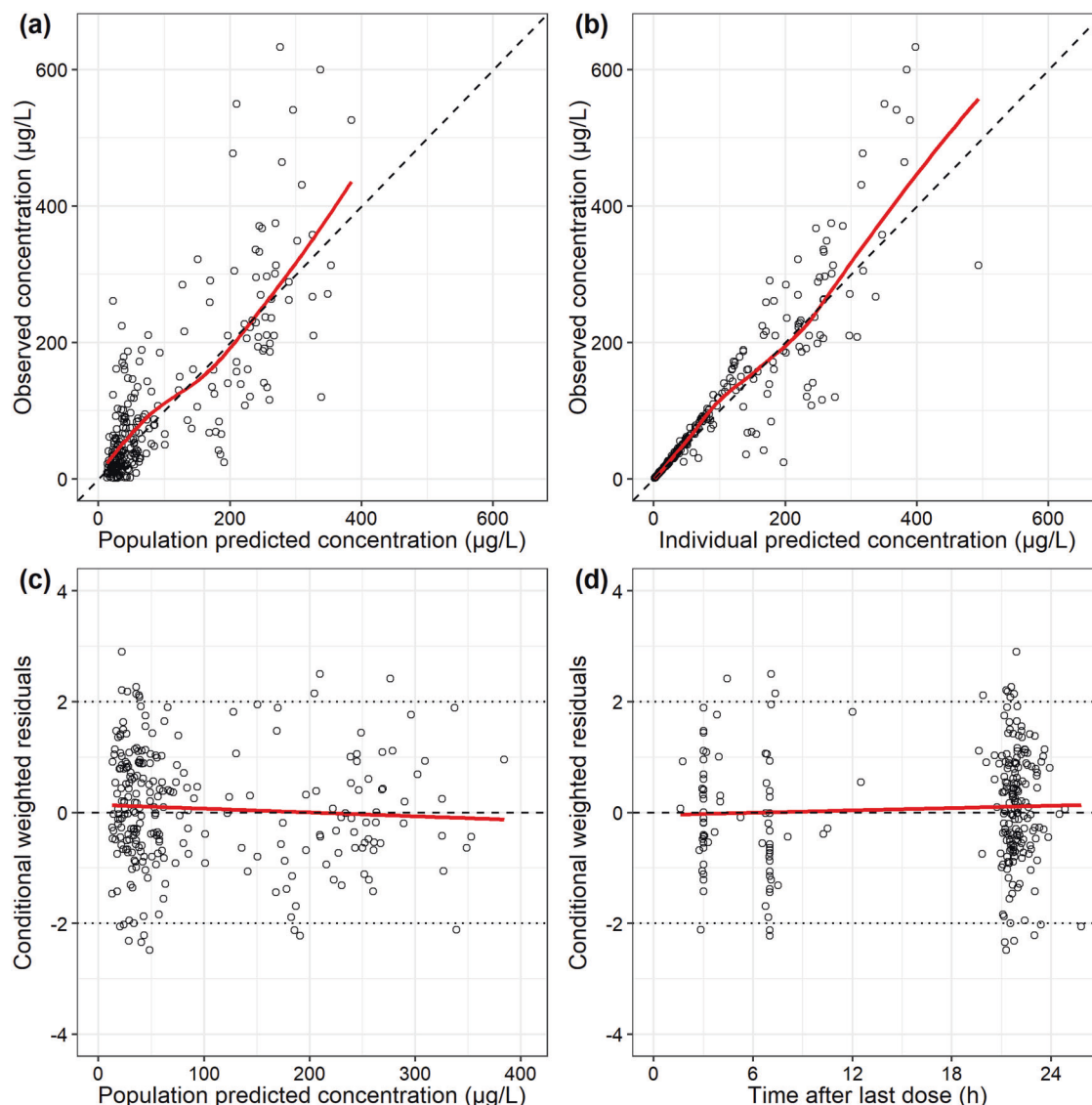
Population PK-PD of rivaroxaban in NVAF patients
XQ Liu et al.

2728

Fig. 1 **Goodness-of-fit plots of the final population pharmacokinetic model.** (**a**) Observed rivaroxaban concentration (DV) *versus* population predicted concentration (PRED); (**b**) DV *versus* individual predicted concentration (IPRED); (**c**) conditional weighted residuals (CWRES) *versus* PRED; (**d**) CWRES *versus* time after last dose.

values from the resampling dataset were within ±3% of the original estimates for all PK-PD parameters, as shown in Table 3.

VPC showed that the median and 95% confidence intervals based on model-based PK-PD predictions were consistent with the observed data (Fig. 3).

Model-informed precision dosing
PK exposure in Chinese, Japanese, and Caucasian patients based on the established model as well as previous reports are shown in Fig. 4. For patients with normal renal function (eGFR or CrCl, 80 mL/min) at a 20 mg dose, the $AUC_{24,ss}$ increased by 31% in Chinese patients compared to that in Caucasian patients. When reducing this to a 15 mg dose for Chinese patients, the $AUC_{24,ss}$ was almost comparable with that in Caucasian patients taking 20 mg (Fig. 4a), and the probability of target attainment was ~85%. Compared to that in Chinese patients with normal renal function taking a 15 mg dose, the $AUC_{24,ss}$ in patients with mildly (eGFR or CrCl, 50 mL/min) or moderately (eGFR or CrCl, 30 mL/min) impaired renal function increased by 29% and 73%, respectively (Fig. 4b, c). For Chinese patients with moderately impaired renal function, reducing the dose to

10 mg might lead to values more comparable to the patients with normal renal function.

The 15-mg dose was set as the standard dose for typical patients in the following analysis. The reference population was defined as male patients aged 70 years, body weight 70 kg, eGFR 80 mL/min, TBIL 12 μmol/L, and receiving rivaroxaban 15 mg q24h. The reference range of $AUC_{24,ss}$ (5th–95th percentiles) was 1716–5390 μg·h·L^{-1}, which was similar to the range in Caucasian populations taking 20 mg q24h reported in a previous study (1860–5434 μg·h·L^{-1}) [3]. The reference of $PT_{ave,ss}$ (5th–95th percentiles) was 12.9–18.3 s.

When eGFR decreased from 80 mL/min to 50 and 30 mL/min, $AUC_{24,ss}$ increased by ~28.3% and 68.1% at a 15-mg dose, respectively. Patients with eGFR ≥ 50 mL/min may require a dose of 15 mg. For patients with eGFR of 30–49 mL/min, the dose needs to be reduced to 10 mg (Fig. 5a).

Compared with that in a patient (eGFR 80 mL/min, TBIL 12 μmol/L) taking 15 mg q24h, the sole effect of increased TBIL or decreased eGFR was less than 20% for most patients. However, for patients with TBIL of 34 μmol/L and eGFR of 30 mL/min, the change in $PT_{ave,ss}$ was ~25.5%. The change in $PT_{ave,ss}$ could be less

Population PK-PD of rivaroxaban in NVAF patients
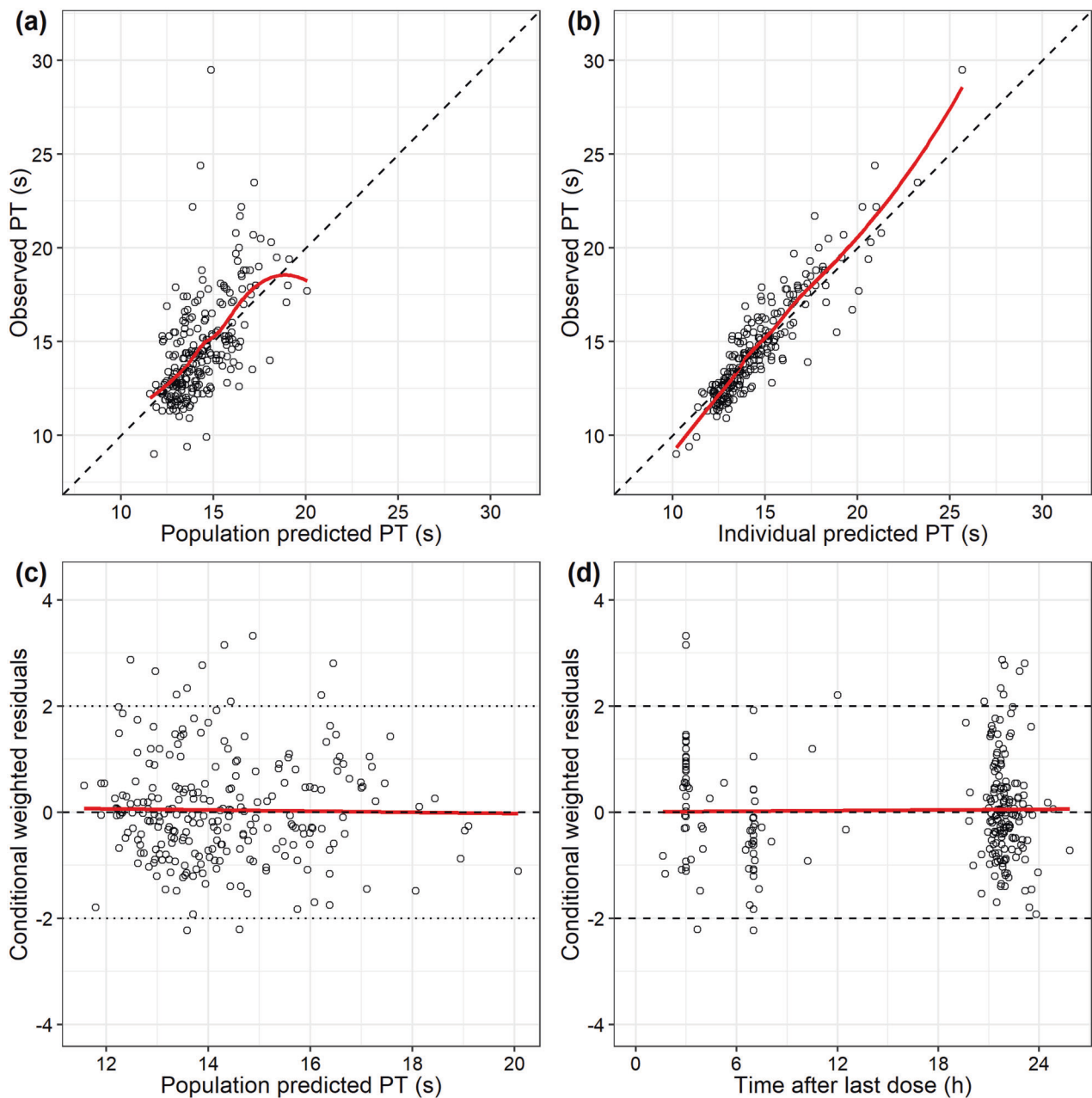XQ Liu et al.

2729

Fig. 2 Goodness-of-fit plots of the final population pharmacodynamic model. (**a**) Observed prothrombin time (PT) versus population predicted PT (PRED); (**b**) observed PT *versus* individual predicted PT; (**c**) conditional weighted residuals (CWRES) versus PRED; (**d**) CWRES versus time after last dose.

than 20% when patients received an adjusted dose based on the eGFR, as previously demonstrated. However, an approximate 18% increase in $PT_{ave,ss}$ was still observed for patients with TBIL of 34 µmol/L and eGFR of 30 mL/min, even though the dose was reduced to 10 mg q24h (Fig. 5b).

DISCUSSION
This is the first study to develop a population PK-PD model of rivaroxaban in Chinese patients with NVAF. The established population PK-PD model comprehensively described the effect of eGFR on CL/F as well as the effect of TBIL and eGFR on the baseline of PT. Exposure in Chinese patients receiving 15 mg q24h of rivaroxaban is similar to that in Caucasian patients taking 20 mg q24h. Patients with eGFR of 30–49 mL/min taking

10 mg have a similar exposure to that in patients with eGFR > 50 mL/min taking 15 mg. These findings support lower rivaroxaban doses in Chinese patients than in Caucasian patients. Moreover, the established PK-PD model indicated that there is a high risk of PT overexposure in patients with TBIL ≥ 34 µmol/L and eGFR ≤ 30 mL/min.

The typical value of CL/F in our study was 5.03 L/h, which is similar to the values estimated in Japanese NVAF patients (4.72–4.73 L/h) [14, 15], but was lower than that in Caucasian NVAF patients (6.10 L/h) [27]. The lower CL/F in the Japanese population than in the Caucasian population taking the same dose of rivaroxaban, which led to higher exposure, can be partly explained by the higher proportion of older age and lower body mass in Japanese patients [14, 15, 38]. These two clinical variables (age and weight) were also reported as significant covariates for
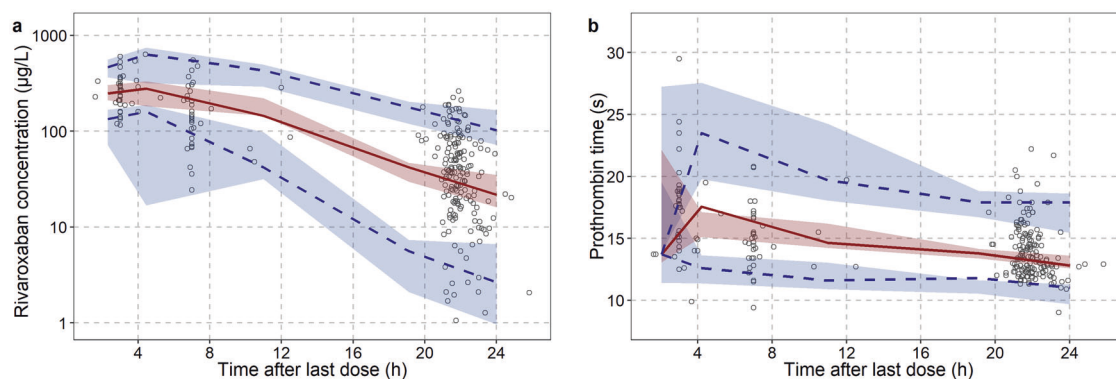
Population PK-PD of rivaroxaban in NVAF patients
XQ Liu et al.

2730

Fig. 3 **Visual predictive check of the final model.** (**a**) Population pharmacokinetic model; (**b**) population pharmacodynamic model. Open circles represent the observed data. Red solid lines and blue dashed lines represent the median and 90% confidence intervals, respectively, of observed data. Red shaded areas represent nonparametric 95% confidence intervals of the median values of model-based predictions; blue shaded areas represent nonparametric 95% confidence intervals of the 5th and 95th percentiles of model-based predictions.

CL/F in a previous population PK model [34]. A similar estimate of typical CL/F was observed between Chinese patients and Japanese patients, and it also may be attributed to the similar demographic characteristics of the two populations (age, 68 versus 72 years; body weight, 68 versus 64 kg; serum creatinine, 0.92 versus 0.9 mg/dL).

Previous studies had investigated the PK and PD of rivaroxaban in healthy Chinese subjects [39, 40]. No studies had been performed to explore the PK and PD of rivaroxaban in NVAF patients with or without renal and hepatic impairment and to assess the rationality of dose regimens. Based on the Monte Carlo simulation, Chinese patients taking 20 mg q24h of rivaroxaban experienced an increase in $AUC_{24,ss}$ compared to that in Caucasian patients, whereas 15 mg q24h of rivaroxaban yielded a similar exposure to that in Caucasian patients. Due to the close PK parameters between the Chinese and Japanese populations, $AUC_{24,ss}$ of these two ethnic groups with 15 mg q24h were also similar. Considering that a lower dose of 15 mg was approved in Japan as a standard dose and that its safety and efficacy have been demonstrated in many clinical studies [12, 20, 21, 41, 42], this may further support applying the low rivaroxaban dose from the Japanese population to the Chinese population.

Our study demonstrated the large effect of renal function on exposure and the requirement of a lower dose for patients with moderate impaired renal function. Compared with patients (eGFR 80 mL/min, TBIL 12 μmol/L) taking 15 mg, those with eGFR 30–49 mL/min experienced an ~29%–68% increase in $AUC_{24,ss}$. This finding was consistent with a previous study in a Caucasian population, which indicated a 1.52-fold (90% confidence interval 1.15–2.01) increase in $AUC_{24,ss}$ for patients with eGFR 30–49 mL/min [43]. The median $AUC_{24,ss}$ of patients with eGFR 30–49 mL/min taking 10 mg were ~2560–3354 μg·h·L^{-1}, which is similar to the exposure of patients with eGFR 80 mL/min taking 15 mg. Therefore, dose reduction is warranted in patients with renal impairment to avoid overexposure.

PT, reflecting the effect of rivaroxaban on coagulation stimulated via the extrinsic pathway of the procoagulant cascade [44, 45], was used as a PD parameter in our study. It was also the most commonly used PD marker in previous population PK-PD studies of rivaroxaban [14, 15, 27, 37, 46–50]. Although there is no well-recognized PD marker for rivaroxaban, PT is regarded as a biomarker to confirm the presence of rivaroxaban [51]. Moreover, PT was reported to be closely correlated with the risk of major bleeding according to the FDA [52], and a prolonged PT also indicates an increased risk of bleeding [53, 54]. Other PD parameters used previously, including activated partial thromboplastin time, prothrombinase-induced clotting time (PiCT) and Heptest [14, 27, 50], lack evidence of clinical relevance till now.

Meanwhile, it should be noted that the international normalized ratio (INR) should not be used to monitor rivaroxaban [51]. When converting PT to INR using the manufacturer-provided generic international sensitivity index (ISI) values, there is more pronounced variability, making it unreliable for clinical monitoring [55, 56]. This is because the ISI was developed from patients treated with warfarin and is not suitable for PT prolonged by factor Xa inhibitors [57].

The estimate of baseline PT in our study (13.9 s) was comparable with previous reports in Japanese patients (11.4–14 s) [14, 15, 37] and non-Japanese patients (11.4–13.9 s) [27, 47–50]. The estimate of slope in our study (0.0133 s·L·μg^{-1}) was similar to the reported value in a study conducted in Japanese NVAF patients using the same PT bioassay (0.0158 s·L·μg^{-1}) [37]. This indicates that there may be no obvious differences in the PT responses between Chinese and Japanese individuals.

In our study, TBIL and eGFR were detected as significant covariates of PT baseline. The effect of liver and kidney function on PT has also been reported in previous studies [15, 27, 47–49]. PT may be prolonged when clotting factors are deficient or inhibited due to other factors such as medication, liver disease, and vitamin K deficiency [44, 45]. Many clotting factors are synthesized by the liver and are reduced when the liver is damaged, which consequently leads to prolonged PT [45]. TBIL level is an important variable in the Child–Pugh score system for assessing the prognosis of chronic liver disease, and it may increase in cholestatic or hepatocellular diseases [23, 58]. The association between eGFR and PT may be explained by the prevalent suboptimal vitamin K status in patients with chronic kidney disease [59, 60]. Regardless, the extent to which PT changes are clinically relevant is still unclear. The overall effect of TBIL and eGFR on PT might be minor, and the maximum change in $PT_{ave,ss}$ was ~26% in our study.

As with the current package insert, from a PK perspective, we also demonstrated the requirement for dose reductions in patients with moderately impaired renal function. Moreover, we found that patients with normal or mildly impaired liver function had a higher PT level, even after dose adjustment based on renal function. Previous studies had explored the effect of impaired renal function or liver function alone based on the PK and/or PD of rivaroxaban and well documented in the package insert [9, 43, 61], but it should be aware that there are patients with both impaired liver and renal function. Although the clinical relevance of an elevated PT is still unclear, clinicians should still pay more attention to these vulnerable patients, considering the relationship between elevated PT and the risk of major bleeding [52, 62].

Several studies have investigated the effect of genetic polymorphisms of *ABCB1* on the PK of rivaroxaban [63–66]. However, only one study with a large sample size ($n = 156$) detected the
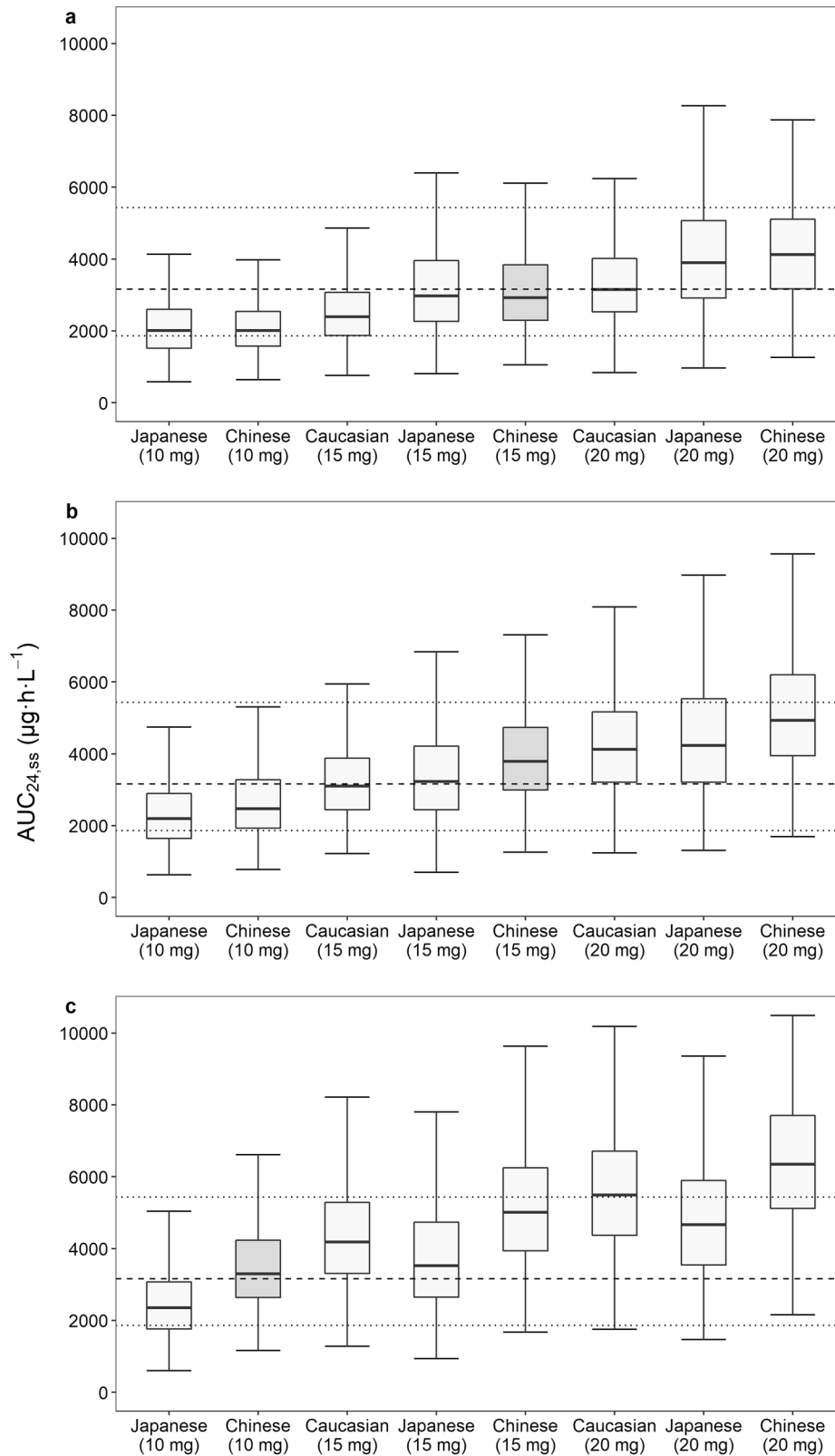
Population PK-PD of rivaroxaban in NVAF patients
XQ Liu et al.

2731

Fig. 4 Comparison of estimated level of pharmacokinetic exposure. The bold horizontal bars represent the median values of estimated $AUC_{24,ss}$. The black dashed and dotted lines represent the median and 5th–95th percentiles of the $AUC_{24,ss}$ for Caucasian patients (CrCl ≥ 50 mL/min, taking 20 mg q24h) as reported by Mueck et al. [3]. Typical patients (**a**) 65 years old, SCr 0.95 mg/dL, eGFR (or CrCl) 80 mL/min, HCT 40.0%; (**b**) 75 years old, SCr 1.5 mg/dL, eGFR (or CrCl) 50 mL/min, HCT 40.0%; (**c**) 85 years old, SCr 2 mg/dL, eGFR (or CrCl) 30 mL/min, HCT 40.0%. The gray boxplot in each panel represents the dose regimen with the highest probability of target attainment for Chinese.

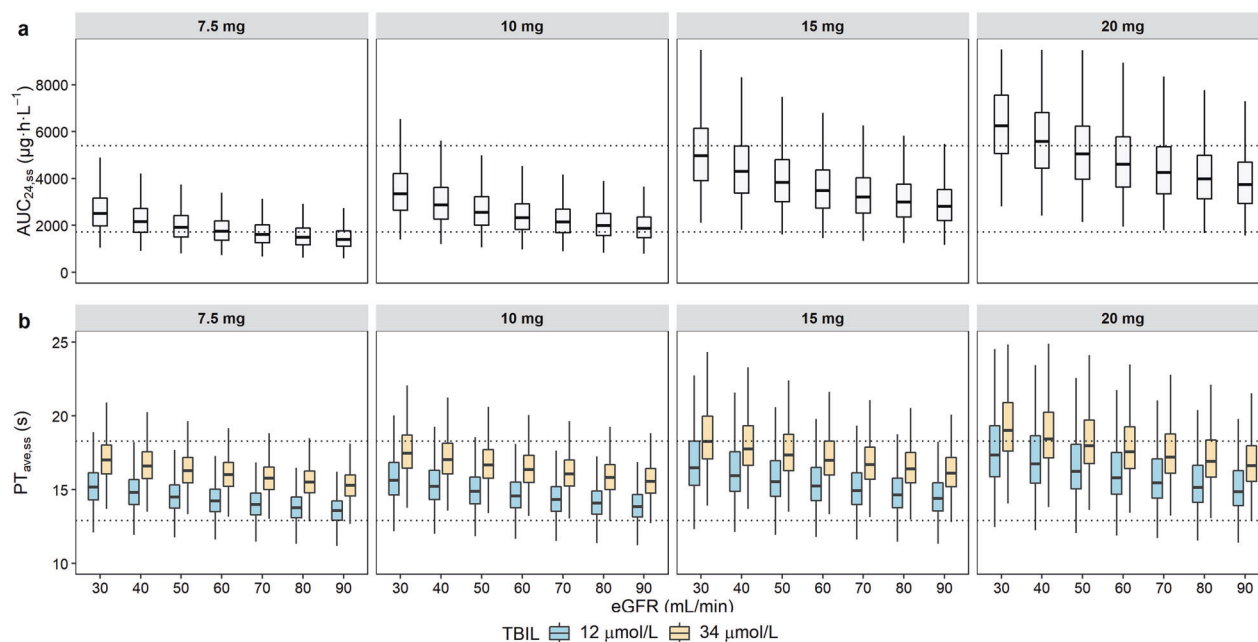Population PK-PD of rivaroxaban in NVAF patients
XQ Liu et al.

2732

Fig. 5 Boxplots of the distribution of simulated area under the concentration-time curve over 24 h and average prothrombin time at steady state based on 7.5, 10, 15, and 20 mg q24h regimens for non-valvular atrial fibrillation patients. The distribution of simulated (**a**) area under the concentration-time curve over 24 h at steady state ($AUC_{24,ss}$); (**b**) average prothrombin time at steady state ($PT_{ave,ss}$). The black dotted lines represent the range of the 5th–95th percentiles of $AUC_{24,ss}$ and $PT_{ave,ss}$ for typical patients (70 years, body weight 70 kg, eGFR 80 mL/min, TBIL 12 µmol/L) with 15 mg q24h of rivaroxaban.

relationship between *ABCB1* rs1128503 variant and rivaroxaban trough concentration ($P < 0.05$) [66]. The inconsistency of the research results indicates that the *ABCB1* genotype may not be a significant covariate for the PK of rivaroxaban. In the present study, the *ABCB1* rs4148738 genotype was statistically significant for CL/F but without clinical relevance (<20%); accordingly, dose adjustment based on genotype does not appear to be warranted. Moreover, our study further found that genetic polymorphisms of *ABCG2* and *CYP3A4/5* had little impact on rivaroxaban clearance.

Our study has several limitations. First, limited samples in the absorption phase were obtained; thus, k_a could not be estimated; instead, we applied values reported in a previous study [15]. In addition, we could not estimate the BSV of V/F and determine the covariates on V/F either, because the majority of collected samples in our study represented the trough concentration. However, CL/F is a more important index for patients with long-term pharmacotherapy, and the CL/F and the impacts of its covariate could be precisely estimated [67]. Second, PT tests might not be the optimal PD marker for rivaroxaban, which limits the interpretation of PT changes. Third, limited patients with eGFR < 30 mL/min and TBIL > 34 µmol/L were included in our study. Our findings may not be extrapolated to this particular population and may require further investigation.

In conclusion, a population PK-PD model of rivaroxaban was developed based on Chinese patients with NVAF. The eGFR and TBIL levels affected the PK-PD characteristics of rivaroxaban. Model-based simulation suggests that 15 mg of rivaroxaban in Chinese patients with normal renal and liver function provided a similar exposure compared with 20 mg in Caucasian patients. A lower dose is recommended for patients with renal impairment to avoid overexposure. Additionally, patients with eGFR ≤ 30 mL/min accompanied by TBIL ≥ 34 µmol/L had a higher PT level, even when the dose was adjusted according to renal function, which requires more attention with respect to the risk of major bleeding. Population PK-PD analyses could provide individualized dosing strategies considering both kidney and liver function in Chinese NVAF patients taking rivaroxaban for stroke prevention.

AUTHOR CONTRIBUTIONS
XQL, ZJ, MKZ, and CLM designed research; XQL, YFZ, HYD, and MMY performed research; XQL, YFZ, MCL contributed new reagents or analytic tools; XQL and ZJ analyzed data; XQL, ZJ, and CLM wrote the paper.

ADDITIONAL INFORMATION
Supplementary information The online version contains supplementary material available at https://doi.org/10.1038/s41401-022-00892-9.

Competing interests: The authors declare no competing interests.

REFERENCES
1. Staerk L, Sherer JA, Ko D, Benjamin EJ, Helm RH. Atrial fibrillation: epidemiology, pathophysiology, and clinical outcomes. Circ Res. 2017;120:1501–17.
2. Chen LY, Chung MK, Allen LA, Ezekowitz M, Furie KL, McCabe P, et al. Atrial fibrillation burden: moving beyond atrial fibrillation as a binary entity: a scientific statement from the American Heart Association. Circulation. 2018;137:e623–e44.
3. Mueck W, Stampfuss J, Kubitza D, Becka M. Clinical pharmacokinetic and pharmacodynamic profile of rivaroxaban. Clin Pharmacokinet. 2014;53:1–16.
4. Steffel J, Collins R, Antz M, Cornu P, Desteghe L, Haeusler KG, et al. 2021 European Heart Rhythm Association practical guide on the use of non-vitamin K antagonist oral anticoagulants in patients with atrial fibrillation. Europace. 2021;23:1612–76.
5. Maggioni AP, Dondi L, Andreotti F, Pedrini A, Calabria S, Ronconi G, et al. Four-year trends in oral anticoagulant use and declining rates of ischemic stroke among 194,030 atrial fibrillation patients drawn from a sample of 12 million people. Am Heart J. 2020;220:12–9.
6. Kubitza D, Becka M, Wensing G, Voith B, Zuehlsdorf M. Safety, pharmacodynamics, and pharmacokinetics of BAY 59-7939-an oral, direct Factor Xa inhibitor-after multiple dosing in healthy male subjects. Eur J Clin Pharmacol. 2005;61:873–80.
7. Kubitza D, Becka M, Voith B, Zuehlsdorf M. Wensing G. Safety, pharmacodynamics, and pharmacokinetics of single doses of BAY 59-7939, an oral, direct factor Xa inhibitor. Clin Pharmacol Ther. 2005;78:412–21.

Population PK-PD of rivaroxaban in NVAF patients
XQ Liu et al.

2733

8. Stampfuss J, Kubitza D, Becka M, Mueck W. The effect of food on the absorption and pharmacokinetics of rivaroxaban. Int J Clin Pharmacol Ther. 2013;51:549–61.

9. XARELTO insert package [homepage on the Internet]. Food and Drug Administration [updated 2021 Dec; cited 2022 Jan 10]. Available from: https://www.accessdata.fda.gov/drugsatfda_docs/label/2021/215859s000lbl.pdf.

10. Gnoth MJ, Buetehorn U, Muenster U, Schwarz T, Sandmann S. In vitro and in vivo P-glycoprotein transport characteristics of rivaroxaban. J Pharm Exp Ther. 2011;338:372–80.

11. Zhang S, Yang YM, Huang CX, Huang DJ, Cao KJ, Zhu J, et al. Guideline of stroke prevention in Chinese patients with atrial fibrillation (2017). Chin J Card arrhyth 2018;22:17–30. Chinese

12. Hori M, Matsumoto M, Tanahashi N, Momomura S-I, Uchiyama S, Goto S, et al. Rivaroxaban vs. warfarin in Japanese patients with atrial fibrillation - the J-ROCKET AF study. Circ J. 2012;76:2104–11.

13. Hori M, Matsumoto M, Tanahashi N, Momomura S, Uchiyama S, Goto S, et al. Safety and efficacy of adjusted dose of rivaroxaban in Japanese patients with non-valvular atrial fibrillation: subanalysis of J-ROCKET AF for patients with moderate renal impairment. Circ J. 2013;77:632–8.

14. Tanigawa T, Kaneko M, Hashizume K, Kajikawa M, Ueda H, Tajiri M, et al. Model-based dose selection for phase III rivaroxaban study in Japanese patients with non-valvular atrial fibrillation. Drug Metab Pharmacokinet. 2013;28:59–70.

15. Kaneko M, Tanigawa T, Hashizume K, Kajikawa M, Tajiri M, Mueck W. Confirmation of model-based dose selection for a Japanese phase III study of rivaroxaban in non-valvular atrial fibrillation patients. Drug Metab Pharmacokinet. 2013;28:321–31.

16. Patel MR, Mahaffey KW, Garg J, Pan G, Singer DE, Hacke W, et al. Rivaroxaban versus warfarin in nonvalvular atrial fibrillation. N. Engl J Med. 2011;365:883–91.

17. Cho MS, Yun JE, Park JJ, Kim YJ, Lee J, Kim H, et al. Pattern and impact of off-label underdosing of non-vitamin K antagonist oral anticoagulants in patients with atrial fibrillation who are indicated for standard dosing. Am J Cardiol. 2020;125:1332–8.

18. Jeong HK, Lee KH, Park HW, Yoon NS, Kim MC, Lee N, et al. Real world comparison of rivaroxaban and warfarin in Korean patients with atrial fibrillation: propensity matching cohort analysis. Chonnam Med J 2019;55:54–61.

19. Chan YH, Kuo CT, Yeh YH, Chang SH, Wu LS, Lee HF, et al. Thromboembolic, bleeding, and mortality risks of rivaroxaban and dabigatran in Asians with non-valvular atrial fibrillation. J Am Coll Cardiol. 2016;68:1389–401.

20. Chan YH, Lee HF, Wang CL, Chang SH, Yeh CH, Chao TF, et al. Comparisons of rivaroxaban following different dosage criteria (ROCKET AF or J-ROCKET AF trials) in Asian patients with atrial fibrillation. J Am Heart Assoc. 2019;8:e013053.

21. Lee HF, Chan YH, Tu HT, Kuo CT, Yeh YH, Chang SH, et al. The effectiveness and safety of low-dose rivaroxaban in Asians with non-valvular atrial fibrillation. Int J Cardiol. 2018;261:78–83.

22. Kirchhof P, Benussi S, Kotecha D, Ahlsson A, Atar D, Casadei B, et al. 2016 ESC Guidelines for the management of atrial fibrillation developed in collaboration with EACTS. Eur Heart J. 2016;37:2893–962.

23. Pugh RN, Murray-Lyon IM, Dawson JL, Pietroni MC, Williams R. Transection of the oesophagus for bleeding oesophageal varices. Br J Surg. 1973;60:646–9.

24. Cockcroft DW, Gault MH. Prediction of creatinine clearance from serum creatinine. Nephron 1976;16:31–41.

25. Lip GY, Nieuwlaat R, Pisters R, Lane DA, Crijns HJ. Refining clinical risk stratification for predicting stroke and thromboembolism in atrial fibrillation using a novel risk factor-based approach: the euro heart survey on atrial fibrillation. Chest 2010;137:263–72.

26. Pisters R, Lane DA, Nieuwlaat R, de Vos CB, Crijns HJ, Lip GY. A novel user-friendly score (HAS-BLED) to assess 1-year risk of major bleeding in patients with atrial fibrillation: the Euro Heart Survey. Chest. 2010;138:1093–100.

27. Girgis IG, Patel MR, Peters GR, Moore KT, Mahaffey KW, Nessel CC, et al. Population pharmacokinetics and pharmacodynamics of rivaroxaban in patients with non-valvular atrial fibrillation: results from ROCKET AF. J Clin Pharm. 2014;54:917–27.

28. Zhang YF, Liu XQ, Wang Y, Xu X, Zhong MK, Zhang P, et al. Development and validation of an ultra high performance liquid chromatography with tandem mass spectrometry method for the simultaneous quantification of direct oral anticoagulants in human plasma. J Chromatogr B Anal Technol Biomed Life Sci. 2021;1182:122952.

29. User manual | Thromborel® S [homepage on the Internet]. SIEMENS [updated 2016 Feb 7; cited 2021 Sep 30]. Available from: https://dokumen.tips/documents/insert-de-tp-thromborel-s.html.

30. Kawakami T, Backstrom N, Burri R, Husby A, Olason P, Rice AM, et al. Estimation of linkage disequilibrium and interspecific gene flow in Ficedula flycatchers by a newly developed 50k single-nucleotide polymorphism array. Mol Ecol Resour. 2014;14:1248–60.

31. Pettersson FH, Anderson CA, Clarke GM, Barrett JC, Cardon LR, Morris AP, et al. Marker selection for genetic case-control association studies. Nat Protoc. 2009;4:743–52.

32. Zhang L, Beal SL, Sheiner LB. Simultaneous vs. sequential analysis for population PK/PD data I: best-case performance. J Pharmacokinet Pharmacodyn. 2003;30:387–404.

33. Zhang L, Beal SL, Sheinerz LB. Simultaneous vs. sequential analysis for population PK/PD data II: robustness of methods. J Pharmacokinet Pharmacodyn. 2003;30:405–16.

34. Willmann S, Zhang L, Frede M, Kubitza D, Mueck W, Schmidt S, et al. Integrated population pharmacokinetic analysis of rivaroxaban across multiple patient populations. CPT: Pharmacomet Sys Pharm. 2018;7:309–20.

35. Holford NH. A size standard for pharmacokinetics. Clin Pharmacokinet. 1996;30:329–32.

36. Stevens LA, Claybon MA, Schmid CH, Chen J, Horio M, Imai E, et al. Evaluation of the Chronic Kidney Disease Epidemiology Collaboration equation for estimating the glomerular filtration rate in multiple ethnicities. Kidney Int. 2011;79:555–62.

37. Suzuki S, Yamashita T, Kasai H, Otsuka T, Sagara K. An analysis on distribution and inter-relationships of biomarkers under rivaroxaban in Japanese patients with non-valvular atrial fibrillation (CVI ARO 1). Drug Metab Pharmacokinet. 2018;33:188–93.

38. Hori M, Kajikawa M. The J-ROCKET AF Study: a matter of ethnicity or a matter of weight? Reply. Circ J. 2013;77:2637.

39. Zhao X, Sun P, Zhou Y, Liu Y, Zhang H, Mueck W, et al. Safety, pharmacokinetics and pharmacodynamics of single/multiple doses of the oral, direct Factor Xa inhibitor rivaroxaban in healthy Chinese subjects. Br J Clin Pharm. 2009;68:77–88.

40. Jiang J, Hu YF, Zhang JY, Yang JL, Mueck W, Kubitza D, et al. Safety, pharmacokinetics and pharmacodynamics of single doses of rivaroxaban - an oral, direct factor Xa inhibitor - in elderly Chinese subjects. Thromb Haemost. 2010;103:234–41.

41. Shimokawa H, Yamashita T, Uchiyama S, Kitazono T, Shimizu W, Ikeda T, et al. The EXPAND study: efficacy and safety of rivaroxaban in Japanese patients with non-valvular atrial fibrillation. Int J Cardiol. 2018;258:126–32.

42. Ikeda T, Ogawa S, Kitazono T, Nakagawara J, Minematsu K, Miyamoto S, et al. Real-world safety and effectiveness of rivaroxaban using Japan-specific dosage during long-term follow-up in patients with atrial fibrillation: XAPASS. PLoS One. 2021;16:e0251325.

43. Kubitza D, Becka M, Mueck W, Halabi A, Maatouk H, Klause N, et al. Effects of renal impairment on the pharmacokinetics, pharmacodynamics and safety of rivaroxaban, an oral, direct Factor Xa inhibitor. Br J Clin Pharm. 2010;70:703–12.

44. Kamal AH, Tefferi A, Pruthi RK. How to interpret and pursue an abnormal prothrombin time, activated partial thromboplastin time, and bleeding time in adults. Mayo Clin Proc. 2007;82:864–73.

45. Palta S, Saroa R, Palta A. Overview of the coagulation system. Indian J Anaesth. 2014;58:515–23.

46. Mueck W, Borris LC, Dahl OE, Haas S, Huisman MV, Kakkar AK, et al. Population pharmacokinetics and pharmacodynamics of once-and twice-daily rivaroxaban for the prevention of venous thromboembolism in patients undergoing total hip replacement. Thromb Haemost. 2008;100:453–61.

47. Mueck W, Eriksson BI, Bauer KA, Borris L, Dahl OE, Fisher WD, et al. Population pharmacokinetics and pharmacodynamics of rivaroxaban-an oral, direct factor Xa inhibitor-in patients undergoing major orthopaedic surgery. Clin Pharmacokinet. 2008;47:203–16.

48. Mueck W, Lensing AW, Agnelli G, Decousus H, Prandoni P, Misselwitz F. Rivaroxaban: population pharmacokinetic analyses in patients treated for acute deep-vein thrombosis and exposure simulations in patients with atrial fibrillation treated for stroke prevention. Clin Pharmacokinet. 2011;50:675–86.

49. Xu XS, Moore K, Burton P, Stuyckens K, Mueck W, Rossenu S, et al. Population pharmacokinetics and pharmacodynamics of rivaroxaban in patients with acute coronary syndromes. Br J Clin Pharm. 2012;74:86–97.

50. Zdovc J, Petre M, Pišlar M, Repnik K, Mrhar A, Vogrin M, et al. Downregulation of ABCB1 gene in patients with total hip or knee arthroplasty influences pharmacokinetics of rivaroxaban: a population pharmacokinetic-pharmacodynamic study. Eur J Clin Pharm. 2019;75:817–24.

51. Samama MM, Contant G, Spiro TE, Perzborn E, Le Flem L, Guinet C, et al. Laboratory assessment of rivaroxaban: a review. Thromb J 2013;11:11.

52. Eikelboom JW, Quinlan DJ, Hirsh J, Connolly SJ, Weitz JI. Laboratory monitoring of non-vitamin K antagonist oral anticoagulant use in patients with atrial fibrillation: a review. JAMA Cardiol. 2017;2:566–74.

53. Nakano Y, Kondo T, Osanai H, Murase Y, Nakashima Y, Asano H, et al. Clinical usefulness of measuring prothrombin time and soluble fibrin levels in Japanese patients with atrial fibrillation receiving rivaroxaban. J Cardiol. 2015;65:185–90.

54. Woodruff AE, Wovkulich MM, Mogle BT, Hassan AK. Association between prothrombin time and bleeding in hospitalized patients receiving rivaroxaban. Am J Health Syst Pharm. 2018;75:1783–9.

55. Barrett YC, Wang Z, Frost C, Shenker A. Clinical laboratory measurement of direct factor Xa inhibitors: anti-Xa assay is preferable to prothrombin time assay. Thromb Haemost. 2010;104:1263–71.

2734

56. Smith SA, Morrissey JH. Thromboplastin composition affects the sensitivity of prothrombin time (PT) clotting tests to direct Factor Xa inhibitors. [abstract]. Blood (ASH Annual Meeting Abstracts). 2007; 111: Abstract 928.

57. Zhang J, Toupin D, Lebel MC, Blostein M. Development of an INR for rivaroxaban monitoring using plasma samples from patients. Thromb Res. 2020;187:122–4.

58. Kwo PY, Cohen SM, Lim JK. ACG clinical guideline: evaluation of abnormal liver chemistries. Am J Gastroenterol. 2017;112:18–35.

59. Holden RM, Morton AR, Garland JS, Pavlov A, Day AG, Booth SL. Vitamins K and D status in stages 3-5 chronic kidney disease. Clin J Am Soc Nephrol. 2010;5:590–7.

60. Cozzolino M, Mangano M, Galassi A, Ciceri P, Messa P, Nigwekar S. Vitamin K in chronic kidney disease. Nutrients 2019;11:168.

61. Kubitza D, Roth A, Becka M, Alatrach A, Halabi A, Hinrichsen H, et al. Effect of hepatic impairment on the pharmacokinetics and pharmacodynamics of a single dose of rivaroxaban, an oral, direct Factor Xa inhibitor. Br J Clin Pharm. 2013;76:89–98.

62. Douxfils J, Ageno W, Samama CM, Lessire S, Ten Cate H, Verhamme P, et al. Laboratory testing in patients treated with direct oral anticoagulants: a practical guide for clinicians. J Thromb Haemost. 2018;16:209–19.

63. Nakagawa J, Kinjo T, Iizuka M, Ueno K, Tomita H, Niioka T. Impact of gene polymorphisms in drug-metabolizing enzymes and transporters on trough concentrations of rivaroxaban in patients with atrial fibrillation. Basic Clin Pharm Toxicol. 2021;128:297–304.

64. Gouin-Thibault I, Delavenne X, Blanchard A, Siguret V, Salem JE, Narjoz C, et al. Interindividual variability in dabigatran and rivaroxaban exposure: contribution of ABCB1 genetic polymorphisms and interaction with clarithromycin. J Thromb Haemost. 2017;15:273–83.

65. Sychev D, Minnigulov R, Bochkov P, Ryzhikova K, Yudina I, Lychagin A, et al. Effect of CYP3A4, CYP3A5, ABCB1 gene polymorphisms on rivaroxaban pharmacokinetics in patients undergoing total hip and knee replacement surgery. High Blood Press Cardiovasc Prev. 2019;26:413–20.

66. Wang Y, Chen M, Chen H, Wang F. Influence of ABCB1 gene polymorphism on rivaroxaban blood concentration and hemorrhagic events in patients with atrial fibrillation. Front Pharm. 2021;12:639854.

67. Holford NH, Buclin T. Safe and effective variability-a criterion for dose individualization. Ther Drug Monit. 2012;34:565–8.